

Spectroscopic orbital elements for the helium-rich subdwarf binary PG 1544+488

H. T. Şener^{1★} and C. S. Jeffery^{1,2}

¹Armagh Observatory, College Hill, Armagh BT61 9DG, UK

²Trinity College Dublin, College Green, Dublin 2, Ireland

Accepted 2014 February 26. Received 2014 February 21; in original form 2014 January 28

ABSTRACT

PG 1544+488 is an exceptional short-period spectroscopic binary containing *two* subdwarf B stars. It is *also* exceptional because the surfaces of both components are extremely helium-rich. We present a new analysis of spectroscopy of PG 1544+488 obtained with the William Herschel Telescope. We obtain improved orbital parameters and atmospheric parameters for each component. The orbital period $P = 0.496 \pm 0.002$ d, dynamical mass ratio $M_B/M_A = 0.911 \pm 0.015$ and spectroscopic radius ratio $R_B/R_A = 0.939 \pm 0.004$ indicate a binary consisting of nearly identical twins. The data are insufficient to distinguish any difference in surface composition between the components, which are slightly metal-poor (1/3 solar) and carbon-rich (0.3 per cent by number). The latter indicates that the hotter component, at least, has ignited helium. The best theoretical model for the origin of PG 1544+488 is by the ejection of a common envelope from a binary system in which both components are giants with helium cores of nearly equal mass. Since precise tuning is necessary to yield two helium cores of similar masses at the same epoch, the mass ratio places very tight constraints on the dimensions of the progenitor system and on the physics of the common-envelope ejection mechanism.

Key words: binaries: spectroscopic – stars: chemically peculiar – stars: individual: PG 1544+488 – subdwarfs.

1 INTRODUCTION

Hot subdwarfs are faint blue stars located at the blue end of the horizontal branch. They have masses in the range of $0.4\text{--}0.8 M_\odot$ and radii of $\sim 0.1 R_\odot$ and burn helium in their cores. Hot subdwarfs have lost most of their hydrogen envelopes, but most retain a very thin hydrogen atmosphere. After helium core burning they become white dwarfs, neither ascending the asymptotic giant branch nor ejecting planetary nebulae.

Subdwarf B (sdB) stars typically have masses $\sim 0.5 M_\odot$ and very thin hydrogen-rich envelopes with masses $\leq 0.002 M_\odot$ (Heber 1986; Saffer et al. 1994). Approximately 50 per cent of hot subdwarf stars are in binary systems with periods shorter than 30 d (Heber 2009). Their companions are generally white dwarfs or M dwarfs but there might also be some systems with more massive unseen components (Geier et al. 2010). Nearly all have hydrogen-rich surfaces.

However, ~ 5 per cent of hot subdwarfs have helium-rich envelopes (Green, Schmidt & Liebert 1986; Ahmad & Jeffery 2006). According to Groth, Kudritzki & Heber (1985) and Heber (2009),

He-rich sdO stars have convective atmospheres, while He-poor sdO and sdB stars mostly have radiative atmospheres. In most sdB stars, gravitational settling produces a He-poor atmosphere but this is not viable for sdO stars. Justham, Podsiadlowski & Han (2011) suggest that there might be some He-sdB and even He-sdO stars produced as a result of He-rich mergers. These stars might be cool enough to be sdB stars but could still have convective atmospheres.

There are two commonly accepted formation channels to form a *single He-rich* hot subdwarf star. The first, and the dominant mechanism is considered to be the white-dwarf merger channel (Webbink 1984; Iben & Tutukov 1986). The mass of the resulting star lies in the range $0.4\text{--}0.65 M_\odot$ (Podsiadlowski et al. 2008), depending on the mass of the initial white dwarf binary (Han et al. 2002). It is argued that this process actually produces the majority of extremely helium-rich sdO and sdB stars from the merger of two helium white dwarfs (Zhang & Jeffery 2012).

The other method to form a single subdwarf starts with a star near the tip of the first giant branch. If an enhanced stellar wind removes the giant envelope, and the remnant core ignites helium burning, a subdwarf is formed. In this case, the surface composition of the subdwarf may depend on when helium-core ignition occurs relative to the star leaving the giant branch (Sweigart et al. 2004). The later the helium-core flash occurs, the more efficient is the

★ E-mail: tugcasener@gmail.com

‘flash-mixing’ between the helium core and the residual hydrogen envelope.

Remarkably, there are two *double* He-rich hot subdwarfs: PG 1544+488 (Ahmad, Jeffery & Fullerton 2004) and HE 0301–3039 (Lisker et al. 2004). PG 1544+488 is an exceptional binary in many respects because both of its components are He-rich sdB stars. Here, the question is no longer how to form a helium-rich subdwarf, but how to form *two* helium-rich subdwarfs. For normal subdwarfs in binary systems, several evolution channels have been identified (Podsiadlowski et al. 2008). In the case of PG 1544+488 and HE 0301–3039, we first require a scenario to form a close binary containing *two* subdwarfs, and secondly, a scenario which requires both subdwarfs to be *helium-rich*.

1.1 PG 1544+488

PG 1544+488 was first classified by Green (1980) as a DA white dwarf and subsequently re-classified as a hot subdwarf of type sdOD – a ‘cooler subdwarf with ‘pure’ He I absorption in spectra...’ (Green et al. 1986).

Heber et al. (1988) suggested PG 1544+488 to be the prototype of a new class of He-sdB stars and published its spectrum, analysing the He I, C II and C III lines. The derived effective temperature (T_{eff}) and surface gravity ($\log g$) were 31.0 kK and 5.1 [cgs], respectively.

Lanz et al. (2004) performed a spectroscopic analysis using far-ultraviolet (FUV) spectra from FUSE to establish a formation method for He-sdB stars and concluded that ‘PG 1544+488 fully supports the flash-mixing scenario’. An interesting result was the measurement of a large rotational velocity $v \sin i = 100 \text{ km s}^{-1}$ in PG 1544+488, whereas $v \sin i$ was at most 30 km s^{-1} for the other two He-sdBs observed with FUSE.

Up to this point, PG 1544+488 had been deemed to be a single star. Indeed, at low resolution it does not show radial velocity variations. Observing at higher spectral resolution, Ahmad et al. (2004) discovered spectral lines which were split by a varying amount. They subsequently found that the integrated FUV spectrum showed large velocity shifts when re-extracted into short exposure spectra. They therefore identified PG 1544+488 as a spectroscopic binary system composed of two low-mass He-sdB type stars. An initial solution gave an orbital period of 0.482 d and a mass ratio $q = 1.7 \pm 0.2$.

Ahmad et al. (2004) argued that PG 1544+488 must have formed as a result of close binary evolution followed by the ejection of a common envelope (CE). Both stars must have evolved off the main sequence, so that they both have a helium core, and the system subsequently must have passed through a CE phase, including CE ejection, just before helium ignition in the more massive component. Meanwhile, Sweigart et al. (2004) discussed the shallow and deep flash mixing scenarios for He-rich PG 1544+488 and two other stars. Their conclusion was to suggest a deep flash-mixing scenario for PG 1544+488 which considered the hydrogen envelope was mixed deeply into the helium flash layer, and therefore, the surface was heavily diluted by helium and carbon. Justham et al. (2011) studied the formation of binary He-rich subdwarf stars evolved through double-core CE evolution. This results in a close binary system which contains the exposed cores of both original stars. This occurs by the simultaneous ejection of the envelopes of both stars in the binary, spiralling inwards in an envelope composed by the merging of the components’ envelopes.

In view of the extraordinary difficulty of devising an evolutionary scenario that will result in the formation of *two* helium-rich subdwarfs in a short-period binary, it is of utmost importance to

Table 1. Observing log showing the WHT/ISIS run number, the heliocentric Julian date for the mid-point of each observation, orbital phase with the ephemeris of Table 2, and heliocentric radial velocities and errors for each component.

Run	Phase	HJD –245 3510	V_A (km s^{-1})	\pm	V_B (km s^{-1})	\pm
r746618	0.1844	7.4469	59.8	3.3	–117.2	2.4
r746620	0.1983	7.4538	53.3	3.3	–122.3	2.4
r746708	0.2782	7.4934	61.8	3.0	–115.5	2.1
r746710	0.2923	7.5004	68.0	3.3	–114.9	2.3
r746798	0.3707	7.5393	52.1	10.2	–84.2	7.3
r746800	0.3860	7.5469	43.0	3.6	–79.0	2.6
r746877	0.4631	7.5851	6.4	3.4	–40.7	2.5
r746890	0.4784	7.5927	7.1	4.1	–40.1	2.9
r746859	0.5639	7.6351	–58.9	5.2	4.6	3.7
r746962	0.5778	7.6420	–68.8	2.7	19.4	1.9
r746984	0.6535	7.6795	–96.7	3.0	50.3	2.1
r746986	0.6676	7.6865	–96.0	3.1	60.7	2.2
r747003	0.7291	7.7170	–101.3	3.0	69.3	2.1
r747006	0.7434	7.7241	–107.9	3.4	78.3	2.4
r747516	0.1226	8.4080	37.1	2.8	–93.0	2.0
r747518	0.1367	8.4150	42.1	3.4	–99.4	2.4
r747611	0.2278	8.4602	57.1	3.0	–123.3	2.1
r747613	0.2434	8.4679	56.3	2.8	–126.5	2.0
r747714	0.3384	8.5150	63.5	4.3	–83.7	3.1
r747735	0.4644	8.5775	–4.8	4.3	–49.6	3.1
r747737	0.4783	8.5844	–7.9	8.1	–43.0	5.8
r747742	0.6201	8.6547	–87.4	3.6	42.5	2.6
r747745	0.6340	8.6616	–87.3	2.7	49.6	1.9
r747839	0.7473	8.7178	–112.1	4.3	67.9	3.1
r747841	0.7612	8.7247	–105.0	4.2	70.3	3.0

establish the fundamental properties of both components and, in particular, the mass ratio. In the following paper, we extract the 2005 observations of PG 1544+488 (Section 2) and obtain a new orbital solution (Section 3). Spectroscopic quantities are derived for each component (Section 4) and discussed in terms of evolutionary considerations (Section 5). Overall conclusions and questions for future work are presented in Section 6.

2 OBSERVATIONS

Observations of PG 1544+488 were obtained by Amir Ahmad with the William Herschel Telescope dual beam ISIS spectrograph on the nights of 2005 May 26 and 27.¹ Three wavelength regions centred at 6815 Å (red), 4700 Å (long blue) and 4151 Å (short blue) with a mean dispersion of 0.22 Å per channel were observed approximately once every hour with two exposures each of 600 s. A list of the red observations is shown in Table 1. Data reduction followed standard procedures including debiasing, cosmic ray removal, flat fielding, sky subtraction, wavelength calibration, scrunching and normalization using STARLINK packages (<http://starlink.jach.hawaii.edu>). At quadrature, both components are easily resolved (Fig. 1). A typical line profile shows a strong and a weak component, which we shall label A and B, respectively.

To measure radial velocities from red spectra, the He I 6678.15 Å line was isolated. A baseline and two Gaussians were fitted to each spectral line using the IDL procedure MPFIT (Markwardt 2009). Gaussian widths and intensity ratios were fixed in order to keep

¹ A preliminary analysis based on these observations exists only in abstract form (Ahmad et al. 2007a).

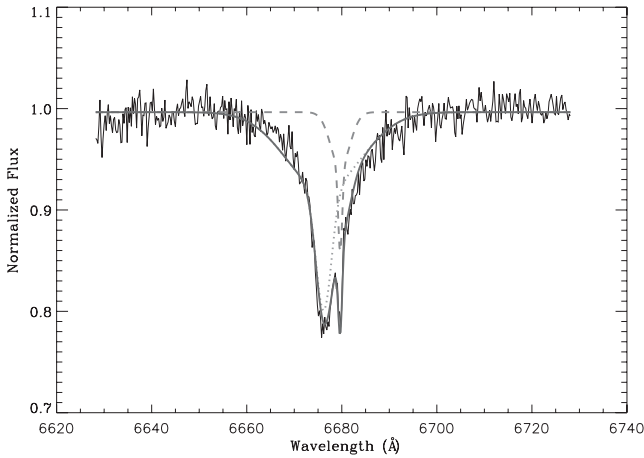


Figure 1. A section of red spectrum r746986 showing the He I 6678 absorption line, together with the Gaussian fit used to measure the radial velocities of the components. In this example, the stronger blue-shifted component (A: dotted) has a heliocentric radial velocity $-96.0 \pm 3.1 \text{ km s}^{-1}$, the weaker red-shifted component (B: dashed) has a radial velocity $60.7 \pm 2.2 \text{ km s}^{-1}$. The bold line is the combination of both components.

consistency between the fits to each spectrum. Radial velocities were directly calculated from the centroids of each component. Fig. 1 shows a sample spectrum and the Gaussian fits to components A and B which led us to determine the radial velocities of the components as given in Table 1.

Due to the lower resolution of the blue spectra, the line splitting and shifts are harder to measure. Therefore, computing and measuring radial velocities from the cross-correlation function was preferred to fitting Gaussians to the line profiles. A template spectrum was produced by calculating the mean of four spectra close to conjunction given in Table 3. A mask was applied to exclude regions between 4500–4670 Å and 4730–4840 Å in a way to include strong lines. Each spectrum was cross-correlated with the template. The radial velocity shifts were measured by fitting a parabola to the peaks of the resulting cross-correlation function. To measure the template velocity, the template spectrum was cross-correlated with a local thermodynamic equilibrium (LTE) model spectrum of $T_{\text{eff}} = 30\,000 \text{ K}$, $\log g = 5.0$ and helium abundance $n_{\text{He}} = 0.99$ (Behara & Jeffery 2006). Only velocities obtained close to quadrature were deemed reliable, and these were used only in the spectroscopic analysis discussed in Section 4.

3 ORBITAL SOLUTION

Assuming a circular orbit, the radial velocity curve is solved by fitting a sinusoid plus a constant in the form

$$V_{\text{rad}} = \gamma + K \sin(2\pi f(t - T_0)), \quad (1)$$

where $K = (2\pi a \sin i)/P$ is the semi-amplitude of the velocity curve, γ is the systemic velocity of the system, a is the semimajor axis of the orbit, P is the orbital period and the epoch T_0 is a time of conjunction. The method used a gradient-expansion algorithm to compute a weighted least-squares fit to the observations (IDL function CURVEFIT); weights were the inverse of the measurement errors. The quality of the observational data is such that we have assumed a circular orbit.

Orbital solutions which included measurements from the blue spectra and radial velocities from the analysis of Ahmad et al. (2004) were attempted but, these seriously degraded the quality of

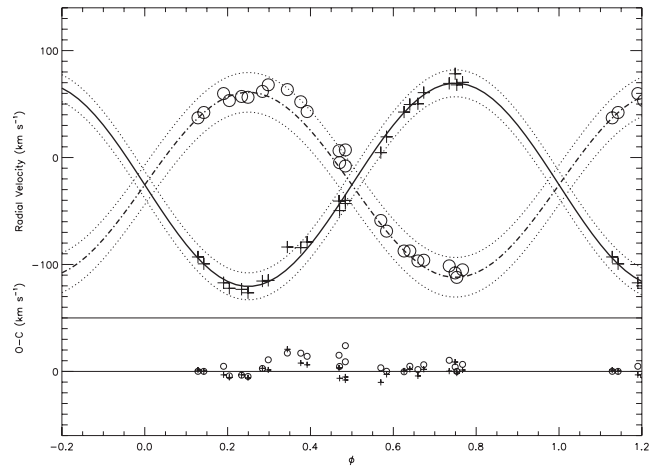


Figure 2. The orbital solution for PG 1544+488 obtained using the 2005 He I 6678 observations. Plus signs represent the primary component, open circles represent the secondary. The top panel shows the orbital solution and $\pm 2\sigma$ envelope. The bottom panel shows the difference between solution and observation, using the same symbols.

Table 2. Orbital solution for PG 1544+488.

	This study	Ahmad et al. (2004)
T_0 (HJD)	$53\,517.3538 \pm 0.0099$	
P (d)	0.496 ± 0.002	0.48 ± 0.01
γ (km s^{-1})	-25.5 ± 0.4	-23 ± 4
K_A (km s^{-1})	86.6 ± 0.5	57 ± 4
K_B (km s^{-1})	95.0 ± 0.4	97 ± 10
$q \equiv M_B/M_A$	0.911 ± 0.015	$0.59 \pm 0.07^*$
$a \sin i$ (R_\odot)	1.78 ± 0.011	1.47 ± 0.13
$M_A \sin^3 i$ (M_\odot)	0.161 ± 0.002	0.114 ± 0.021
$M_B \sin^3 i$ (M_\odot)	0.147 ± 0.002	0.067 ± 0.011

* Ahmad et al. (2004) gave $q = M_A/M_B$.

the fit. Consequently, the adopted orbital solution shown in Fig. 2 is that obtained solely from measurements of the He I 6678 line shown in Table 1 and is shown in Table 2. The best-fitting period is $0.496 \pm 0.002 \text{ d}$.

The errors on the orbital elements reported in Table 2 are remarkably small. We have tested their validity in a number of ways. The errors on the velocity semi-amplitudes and systemic velocity were verified by (a) increasing the values of the measurement errors by a factor 3, and (b) splitting the observations into two sets (odd and even data). Test (a) increases the resultant errors by a factor < 1.3 . Test (b) gave half-ranges in K_B and K_A which were 2.5 and 1.5 km s^{-1} , or 6 and 4σ , respectively. We suspect the errors on K_B and K_A are too small by factors of 3 and 2, respectively. The half-range in γ matches σ_γ exactly. The formal error in the orbital period given by CURVEFIT was just 0.0005 d . Tests which omitted various numbers of data and the odd–even test both indicated a larger error $\sigma_P = 0.002 \text{ d}$ should be admitted. Given that the observations cover only just over three pulsation cycles, the formal error in the epoch $\sigma_{T_0} = 0.1 \text{ d}$ is reasonable.

The new orbital solution is compared with that of Ahmad et al. (2004) in Table 2. Apart from the improved precision the only major difference concerns the semi-amplitude of the second component, which is much better resolved in the 2005 observations. The velocity semi-amplitudes give a dynamical mass ratio $q_{\text{dyn}} \equiv M_B/M_A = 0.911 \pm 0.015$, if the errors σ_K are increased by a factor 3,

Table 3. Observing log showing the WHT/ISIS run number, the heliocentric Julian date for the mid-point of each observation, orbital phase with the ephemeris of Table 2, and heliocentric radial velocities and errors for each component. These data were not used for the orbital solution given in Table 2.

Run	Phase	HJD −245 3510	V_A (km s ^{−1})	\pm	V_B (km s ^{−1})	\pm
r746617	0.3378	8.5150	−98.2	4.4	85.3	5.3
r746619	0.3517	8.5219	−112.4	5.3	75.6	3.7
r746709	0.4414	8.5664	−122.6	3.4	59.9	0.9
r746797	0.4638	8.5775	−81.2	3.4	38.2	2.4
r746985	0.7606	8.7247	94.3	8.3	−102.0	5.0

$\sigma_q = 0.023$. The mass ratio is much closer to unity than initially estimated by Ahmad et al. (2004). The higher velocity resolution of the red He I 6678 line and improved phase coverage contribute to the much smaller errors on the new solution. The question remains as to the total mass of either component, since the inclination is not currently available. For either subdwarf to have ignited helium, a minimum mass of some $\sim 0.45 M_\odot$ and hence an inclination of less than 45° would be required, which is not unreasonable.

4 SPECTROSCOPIC PARAMETERS

After determining the orbital parameters, we measured the effective temperature (T_{eff}) and surface gravity ($\log g$) for each component of PG 1544+488. To do this, we identified the five long-blue spectra closest to quadrature in which both components could best be resolved. These are indicated in Table 3 which also shows the velocities obtained by cross-correlation described in Section 2, and including the template and heliocentric corrections.

The observed spectra were then compared with theoretical spectra appropriate for helium-rich sdB stars. Model atmospheres were calculated with STERNE (Behara & Jeffery 2006), which calculates fully-blanketed plane-parallel atmosphere structures in LTE for stars with effective temperatures between 10 000 and 35 000 K and any chemical composition. Emergent spectra are computed with the formal solution code SPECTRUM (Jeffery, Woolf & Pollacco 2001).

Effective temperatures and surface gravities for each component ($T_{A,B}$, $\log g_{A,B}$) were measured by χ^2 minimization from each spectrum of our five spectra sample. For this, we used the spectral-fitting software SFIT (Jeffery et al. 2001). This interpolates in a grid of model spectra to find a best-fitting solution for a single or binary star spectrum. We used model grids with $4.3 < \log T_{\text{eff}} < 4.7$ and $4 < \log g < 6.5$ for various chemical abundances, i.e. relative abundances by number of hydrogen $n_H = [0.0001, 0.001, 0.1]$, and carbon $n_C = [0.001, 0.01, 0.03]$, and overall metallicities of one and one-third times solar. In all cases, the micro-turbulent velocity was assumed to be 5 km s^{-1} as a compromise between JL87 (Ahmad et al. 2007b) and six other He-sdBs (Naslim et al. 2010). Other parameters of the χ^2 solution include the radial velocity, composition and projected rotation velocity $v \sin i$ of each component, as well as the relative radii of each component R_i/R_A .

It was not possible to measure a difference between the chemical compositions of the two components. Since the hydrogen was not detected, the adopted solution for both components has relative abundances (by number) of $n_H = 0.0001$, $n_{\text{He}} = 0.99$ and $n_C = 0.003$. From the weak metal lines in the spectrum, the metallicity is judged to be ≈ 0.3 times the solar value, given in logarithmic units as $[\text{Fe}] = -0.5$ in Table 5. The results for T_{eff} , $\log g$ and R_A/R_B are given in Table 4. The composite and constituent theoretical

Table 4. Physical parameters of PG 1544+488.

	A	B
T_{eff} (K)	$32\,800 \pm 270$	$26\,500 \pm 435$
$\log g$ (cgs)	5.33 ± 0.11	5.35 ± 0.15
R_B/R_A	0.939 ± 0.004	
L_B/L_A	0.376 ± 0.014	
$q \equiv M_B/M_A$	0.923 ± 0.075	
$\log L/M$ (L_\odot/M_\odot)	2.10 ± 0.11	1.70 ± 0.15

spectra are shown in Fig. 3; significant lines are labelled including He I 4387 and 4471 Å which are important in the measurement of surface gravity.

In view of the importance of the carbon abundance to explaining the origin of PG 1544+488, we note that optical lines of C II are notoriously unreliable due to strong departures from LTE. For example, C II multiplet 1 (~ 4730 – 4750 Å) is strong in the models, but undetected in the observations (Fig. 3). This is common in the spectra of early-type hydrogen-deficient stars (Jeffery & Heber 1992). To verify the carbon abundance, we also used the integrated FUV spectrum observed with FUSE on 2002 March 26. Fig. 4 shows the influence of the carbon abundance on the line wings of C III 1176 Å, which demonstrates that a model with $n_C = 0.003$ is substantially better than one with $n_C = 0.001$. Table 5 summarizes our measurements of the chemical composition, and compares them with Lanz et al. (2004).

Since the spectroscopic analysis yields the radius ratio, as well as both temperatures and gravities, it is trivial to deduce the corresponding luminosity and mass ratios, and also the luminosity-to-mass ratio for each component (Table 4). In particular, we find the spectroscopic mass ratio $q_{\text{spec}} \equiv M_B/M_A = 0.923 \pm 0.075$, in excellent agreement with the dynamical mass ratio. Again, PG 1544+488A is the slightly more massive component although, in this case, it is not demonstrably different from unity. It is, however, demonstrably hotter, larger, and more luminous than PG 1544+488B.

Regarding the surface composition, the hydrogen abundance is below the detection threshold of $n_H < 0.001$. (Fig. 5). There is no evidence of H α , H β or H γ distinct from the corresponding He II lines at the same locations. A key question for interpreting the evolutionary status of PG 1544+488 is whether the surface compositions of the two stars are identical. This applies in particular to the carbon abundance. The FUV measurement applies *only* to PG 1544+488A, since the cooler and smaller secondary is invisible at these wavelengths. The blue spectra are not sufficiently well resolved to measure any difference in this case, although the equal-abundance fit to C III 4650 Å looks good.

5 EVOLUTIONARY STATUS OF PG 1544+488

We have established that the spectroscopic binary PG 1544+488 consists of near-twin extremely helium-rich and carbon-rich subdwarfs. The effective temperatures and surface gravities are comparable with other helium-rich subdwarfs (Fig. 6), (Ahmad & Jeffery 2003; Ströer et al. 2007; Naslim et al. 2010). In a g – T_{eff} diagram they are seen to be more luminous than the canonical extended horizontal branch (EHB) for stars with core masses of $0.47 M_\odot$. This is either because they are more massive than $0.47 M_\odot$, or because they evolving on to or away from the EHB, or on to the helium main sequence (He-MS), or because they are simply post-giant branch stars evolving through this part of the g – T_{eff} diagram.

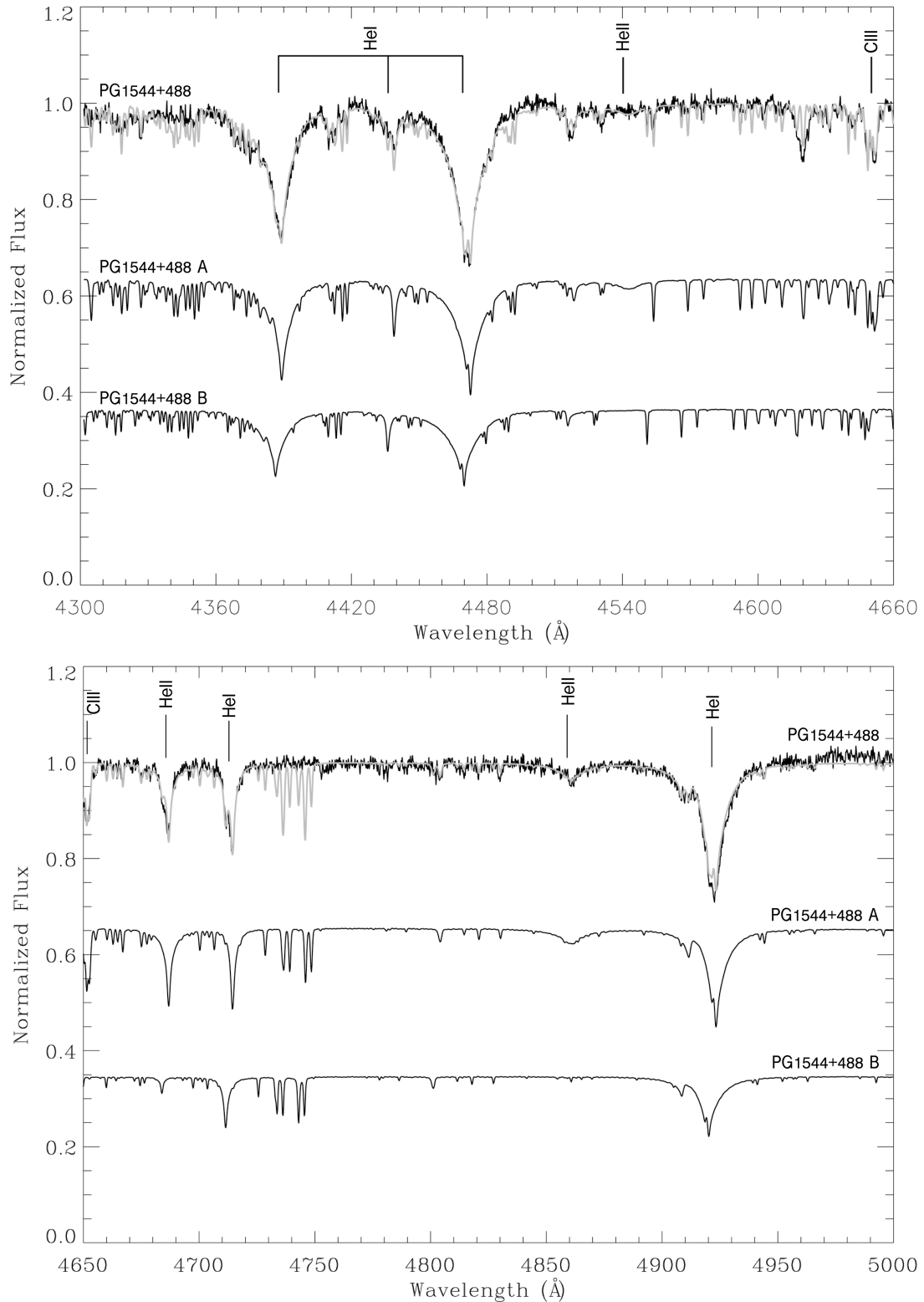


Figure 3. A sample blue spectrum of PG 1544+488 (r676619, Table 3) (dark line) is compared with the combined model fit (grey line), and also showing the relative model contributions due to the individual components. The principal lines due to He I, He II, and C III are identified.

It is therefore desirable to establish whether either or both stars are burning helium, and whether this burning is in the core (He-MS), or in a shell surrounding a degenerate helium core, or in a shell surrounding a carbon–oxygen core. Neither star lies on the theoretical He-MS, so we exclude core helium burning but they are

not inconsistent with the pre-white dwarf evolution tracks of very low mass stars (Driebe et al. 1999).

Since there are no known binaries containing two *hydrogen-rich* sdB stars, the likelihood that we have found such a system in which both components have simultaneously completed core burning and

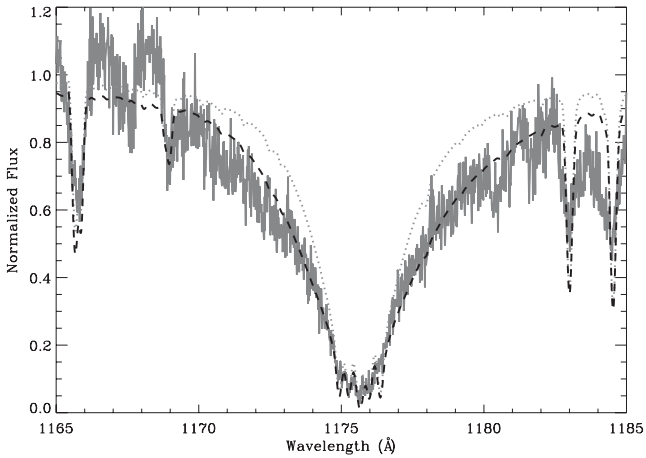


Figure 4. The observed C III 1176 Å line profile from FUSE (solid line) is compared with theoretical profiles calculated for a metallicity 0.3 times solar and for two carbon abundances: $n_C = 0.001$ (dotted) and $n_C = 0.003$ (dashed).

Table 5. Surface abundances.

Abundance	This study	Lanz et al. (2004)
n_H	<0.001	<0.002
n_{He}	0.99 ± 0.01	0.96
n_C	0.003 ± 0.01	0.02
[Fe]	-0.5 ± 0.1	–

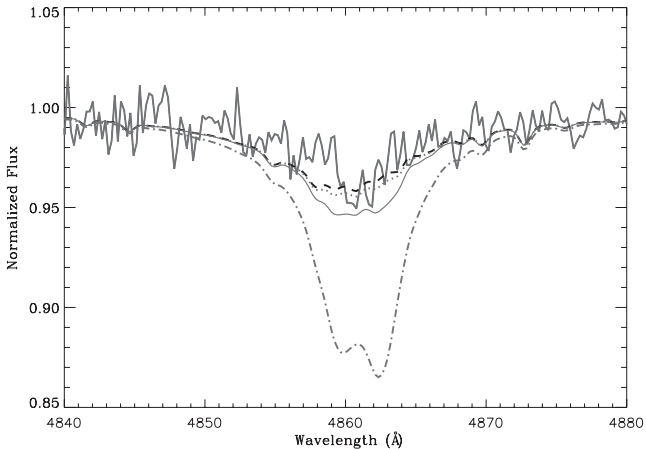


Figure 5. The observed H β 4860 Å line profile from WHT (solid line: r676619, Table 3) is compared with theoretical profiles calculated for different H abundances: $n_H = 0.0001$ (dash), $n_H = 0.0003$ (dot), $n_H = 0.001$ (triple dot-dashed) and $n_H = 0.001$ (dash-dotted).

are evolving away from the EHB and have simultaneously lost their surface hydrogen seems to be remote. The remaining solution is that both components are helium-shell burning stars evolving towards the He-MS.

The next question to address is the formation of hydrogen-deficient carbon-rich shell-burning helium stars. Two major contenders exist.

Brown et al. (2001), Lanz et al. (2004) and Miller Bertolami et al. (2008) construct models for stars which lose most of their hydrogen-rich envelope whilst on the giant branch and shortly before core helium ignition. With the hydrogen shell extinguished,

the degenerate helium core cannot increase in mass, so the star contracts towards the white dwarf track. However, if core contraction can ignite helium (off-centre) to give a *late helium flash*, the star expands to become a yellow giant and then contracts towards the He-MS. If the flash is sufficiently late, flash-driven convection will mix material from the ignition shell through to the stellar surface. Any residual surface hydrogen is ingested (and therefore depleted) and carbon produced in the helium-shell flash can be mixed to the surface.

Another way to produce extremely helium-rich subdwarfs is to merge two helium white dwarfs (Iben 1990; Saio & Jeffery 2000). Zhang & Jeffery (2012) showed that double helium white dwarf mergers can be carbon-rich if the total mass is sufficiently large; the carbon is again produced during helium ignition and mixed to the surface. This scenario is *extremely unlikely* for PG 1544+488, since it would require (a) *two* double-white dwarf mergers within a few thousands of years of one another, and (b) to be preceded by the formation of two compact double-white dwarf binaries in a *quadruple* helium white dwarf system. We reject this as implausible.

Consequently, the late hot flasher model Sweigart et al. (2004) appears to be preferable. However, Justham et al. (2011) point out that the binary nature of PG 1544+488 opens a third possibility. This may occur if both stars are of sufficiently similar mass that they become red giants with nearly identical cores *and* if the envelope of one star overflows its Roche lobe when the more massive star is close to helium ignition. In this case, a CE will form which is effectively the combined envelope of both giants, since both stars overfill their Roche lobes, leading to spiral-in and, ultimately, ejection of the envelope.

Justham et al. (2011) point out that double-core CE evolution has not been proven to exist in nature; PG 1544+488 would be the first such demonstration. Proof of concept might also help to explain the origin of double neutron star binaries. The parameter space which allows double-core evolution to produce a double-hot subdwarf is small, since the secondary must not only have reached the giant branch by the time the primary is ready to ignite helium, it must also be able to ignite helium itself. Justham et al. (2011) discuss two cases. In one: ‘If the secondary is to ignite helium degenerately, its core mass must be within ~ 5 per cent of the core mass at the tip of the giant branch when the envelope is removed (Han et al. 2002). . . . The likelihood . . . is almost negligible’. In the second: ‘stars more massive than . . . will . . . ignite helium non-degenerately even if they lose their envelopes in the Hertzsprung gap. This allows a wider range of parameter space to potentially produce double-hot-subdwarf systems’. For ignition of the secondary, the degenerate case requires the mass ratio of the subdwarfs $q > 0.95$, so is marginally consistent with our measurements but is statistically unlikely. The non-degenerate case is statistically more likely, with allowed subdwarf mass ratios in the range $0.77 < q < 1$. In both cases, the mass difference between the main-sequence progenitors must be less than ~ 0.5 per cent. A theoretical birth rate of one double subdwarf for every 3000 hot subdwarfs from both of these channels is consistent with the uniqueness of PG 1544+488.² Justham et al. (2011) also discuss other channels for the production of dual hot subdwarfs, but state that there is no reason for these to produce stars with extremely hydrogen-poor surfaces. Regrettably, Justham et al. (2011) do not indicate what surface abundances other than hydrogen and helium might be anomalous in either of the viable models. The high

² At present, the other candidate double subdwarf HE0301–3039 (Lisker et al. 2004) remains to be analysed.

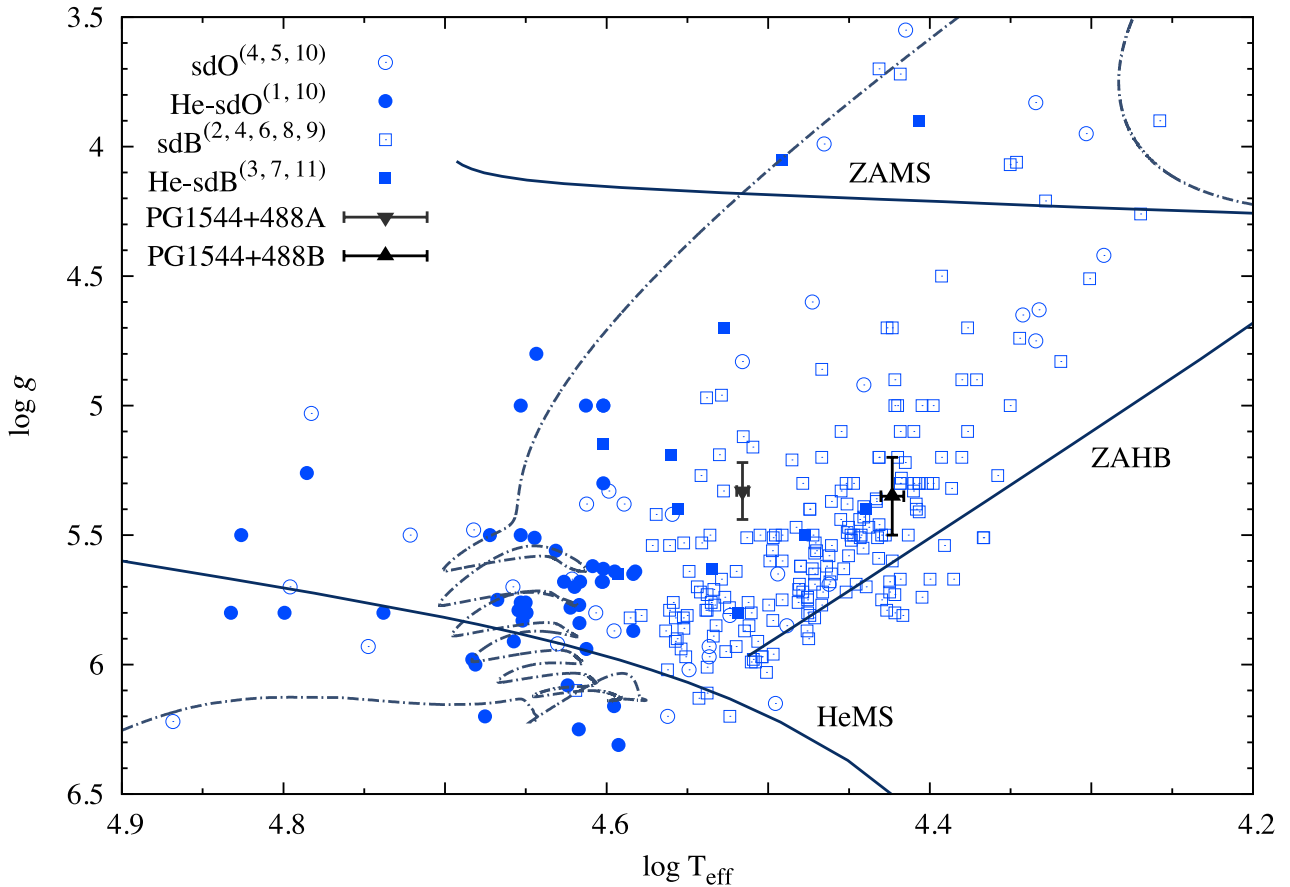


Figure 6. The surface gravity–effective temperature diagram for helium-rich sdB stars showing the positions of PG 1544+488A and PG 1544+488B, other extreme He-rich stars (Ahmad & Jeffery 2003; Ströer et al. 2007; Naslim et al. 2010), the He-MS, the canonical EHB and the evolution track for a late hot flasher (Miller Bertolami et al. 2008). References. 1: Dreizler et al. (1990), 2: Moehler, de Boer & Heber (1990), 3: Vitor et al. (1991), 4: Saffer et al. (1994), 5: Heber et al. (1996), 6: Moehler, Heber & Rupprecht (1997), 7: Jeffery (1998), 8: Maxted et al. (2001), 9: Lisker et al. (2004), 10: Ströer et al. (2007), 11: Naslim et al. (2010).

carbon abundance observed in PG 1544+488 could be produced in a helium shell flash (Miller Bertolami et al. 2008), i.e. following *degenerate* double-core evolution; the question whether high carbon rules out the non-degenerate case remains to be addressed.

6 CONCLUSIONS

The orbital elements of PG 1544+488 have been improved using the best-quality data available. The mean heliocentric velocity of the system (γ) is -27 km s^{-1} , the orbital period is 0.496 d and the mass ratio is close to unity. The large radial-velocity amplitude ($K_1 + K_2 = 177 \text{ km s}^{-1}$) allows the spectra of both components to be resolved and has enabled us to measure the physical properties of both stars independently, despite their overall similarity. Both components are hydrogen-deficient and helium-rich subdwarfs of almost equal mass ($M_B/M_A = 0.911 \pm 0.015$) and radius ($R_B/R_A = 0.939 \pm 0.004$), with an orbital separation of a few solar radii. The best chemical composition which matches both optical and FUV spectra has a metallicity one third of solar and a carbon mass fraction (in the brighter star) of 3 per cent.

Lanz et al. (2004) demonstrated that the carbon abundance plays an important role in determining the best model spectrum for the star, since it dominates the opacity of the atmosphere. Our results indicate a lower carbon abundance than Lanz et al. (2004), possibly due to other systematic differences between the model atmospheres,

but still indicate that at least one star has a carbon-enriched atmosphere.

The results demonstrate that PG 1544+488 consists of near-identical twins, the principal difference being in effective temperature with the slightly more massive component being hotter and hence more luminous. Since there is negligible surface hydrogen, both stars must have completed main-sequence evolution and evolved some distance up the giant branch to the point where a CE was formed and ejected.

More detailed work, probably involving observations at higher spectral resolution and signal-to-noise ratio, will be required to disentangle the spectra of the two components, and to measure their chemical composition more accurately. In particular, measurements of nitrogen, oxygen and other elements will be useful for probing the previous evolution. One problem raised is the origin of the high carbon abundance; Is this really a signature of flash mixing produced by degenerate helium ignition, as Lanz et al. (2004) argue? Are both components carbon-rich? Does this give a clue to the *actual* masses of these stars, and also of their progenitors?

At present, PG 1544+488 represents a unique binary system. Further observations may demonstrate that there are others like it, including HE 0301–3039 for example. Meanwhile, it remains crucial for understanding binary star evolution and it tells us something very important; in a CE binary containing two helium cores of nearly equal mass, the entire hydrogen envelopes of both stars

are ejected. This places a very strong constraint on the physics of the CE ejection mechanism.

ACKNOWLEDGEMENTS

The results presented in this paper are partly based on grids of model spectra computed using model-atmosphere codes written by Natalie Behara (Behara & Jeffery 2006). They are also based on observations obtained by Amir Ahmad and made with the William Herschel Telescope operated on the island of La Palma by the Isaac Newton Group in the Spanish Observatorio del Roque de los Muchachos of the Instituto de Astrofísica de Canarias, and on observations made with the NASA–CNES–CSA Far Ultraviolet Spectroscopic Explorer. FUSE is operated for NASA by the Johns Hopkins University under NASA contract NAS5-32985.

The Armagh Observatory is funded by direct grant from the Northern Ireland Department of Culture, Arts and Leisure.

REFERENCES

- Ahmad A., Jeffery C. S., 2003, *A&A*, 402, 335
 Ahmad A., Jeffery C. S., 2006, *Balt. Astron.*, 15, 139
 Ahmad A., Jeffery C. S., Fullerton A. W., 2004, *A&A*, 418, 275
 Ahmad A., Jeffery C. S., Napiwotzki R., Pandey G., 2007a, in Hartkopf W. I., Harmanec P., Guinan E. F., eds, *Proc. IAU Symp. Vol. 240, Binary Stars as Critical Tools and Tests in Contemporary Astrophysics*. Kluwer, Dordrecht, p. 129
 Ahmad A., Behara N. T., Jeffery C. S., Sahin T., Woolf V. M., 2007b, *A&A*, 465, 541
 Behara N. T., Jeffery C. S., 2006, *A&A*, 451, 643
 Brown T. M., Sweigart A. V., Lanz T., Landsman W. B., Hubeny I., 2001, *ApJ*, 562, 368
 Dreizler S., Heber U., Werner K., Moehler S., de Boer K. S., 1990, *A&A*, 235, 234
 Driebe T., Blöcker T., Schönberner D., Herwig F., 1999, *A&A*, 350, 89
 Geier S., Heber U., Podsiadlowski P., Edelmann H., Napiwotzki R., Kupfer T., Müller S., 2010, *A&A*, 519, A25
 Green R. F., 1980, *ApJ*, 238, 685
 Green R. F., Schmidt M., Liebert J., 1986, *ApJS*, 61, 305
 Groth H. G., Kudritzki R. P., Heber U., 1985, *A&A*, 152, 107
 Han Z., Podsiadlowski P., Maxted P. F. L., Marsh T. R., Ivanova N., 2002, *MNRAS*, 336, 449
 Heber U., 1986, *A&A*, 155, 33
 Heber U., 2009, *ARA&A*, 47, 211
 Heber U., Dreizler S., de Boer K., Moehler S., Richtler T., 1988, *Astron. Ges. Abstr. Ser.*, 1, 16
 Heber U., Dreizler S., Werner K., Engels D., Hagen H.-J., 1996, in Jeffery C. S., Heber U., eds, *ASP Conf. Ser. Vol. 96, Hydrogen Deficient Stars*. Astron. Soc. Pac., San Francisco, p. 241
 Iben I., Jr, 1990, *ApJ*, 353, 215
 Iben I., Jr, Tutukov A. V., 1986, *ApJ*, 311, 753
 Jeffery C. S., 1998, *MNRAS*, 294, 391
 Jeffery C. S., Heber U., 1992, *A&A*, 260, 133
 Jeffery C. S., Woolf V. M., Pollacco D. L., 2001, *A&A*, 376, 497
 Justham S., Podsiadlowski P., Han Z., 2011, *MNRAS*, 410, 984
 Lanz T., Brown T. M., Sweigart A. V., Hubeny I., Landsman W. B., 2004, *ApJ*, 602, 342
 Lisker T., Heber U., Napiwotzki R., Christlieb N., Reimers D., Homeier D., 2004, *Ap&SS*, 291, 351
 Markwardt C. B., 2009, in Bohlender D. A., Durand D., Dowler P., eds, *ASP Conf. Ser. Vol. 411, Astronomical Data Analysis Software and Systems XVIII*. Astron. Soc. Pac., San Francisco, p. 251
 Maxted P. F. L., Heber U., Marsh T. R., North R. C., 2001, *MNRAS*, 326, 1391
 Miller Bertolami M. M., Althaus L. G., Unglaub K., Weiss A., 2008, *A&A*, 491, 253
 Moehler S., de Boer K. S., Heber U., 1990, *A&A*, 239, 265
 Moehler S., Heber U., Rupprecht G., 1997, *A&A*, 319, 109
 Naslim N., Jeffery C. S., Ahmad A., Behara N. T., Şahin T., 2010, *MNRAS*, 409, 582
 Podsiadlowski P., Han Z., Lynas-Gray A. E., Brown D., 2008, in Heber U., Jeffery C. S., Napiwotzki R., eds, *ASP Conf. Ser. Vol. 392, Hot Subdwarf Stars and Related Objects*. Astron. Soc. Pac., San Francisco, p. 15
 Saffer R. A., Bergeron P., Koester D., Liebert J., 1994, *ApJ*, 432, 351
 Saio H., Jeffery C. S., 2000, *MNRAS*, 313, 671
 Ströer A., Heber U., Lisker T., Napiwotzki R., Dreizler S., Christlieb N., Reimers D., 2007, *A&A*, 462, 269
 Sweigart A. V., Lanz T., Brown T. M., Hubeny I., Landsman W. B., 2004, *Ap&SS*, 291, 367
 Viton M., Deleuil M., Tobin W., Prevot L., Bouchet P., 1991, *A&A*, 242, 175
 Webbink R. F., 1984, *ApJ*, 277, 355
 Zhang X., Jeffery C. S., 2012, *MNRAS*, 419, 452

This paper has been typeset from a \LaTeX file prepared by the author.